MAJOR-ELEMENT TRENDS IN CENOZOIC VOLCANITES OF HUNGARY

J.A. Martín-Fernández[1], V. Pawlowsky-Glahn[1], C. Barceló-Vidal[1], L. Ó.Kovács[2], G.P. Kovács[2]
[1]Universitat de Girona, Departament d'Informàtica i Matemàtica Aplicada, Girona, Spain,
carles.barcelo@udg.es, josep.antoni.martin@udg.es, vera.pawlowsky@udg.es
[2]Hungarian Geological Survey, Budapest, Hungary, lajos.okovacs@mgsz.hu, gabor.kovacs@mgsz.hu

1 Introduction: geologic framework

Hungary lies entirely within the Carpatho-Pannonian Region (CPR), a dominant tectonic unit of eastern Central Europe (Fig. 1). The CPR consists of the Pannonian Basin system, and the arc of the Carpathian Mountains surrounding the lowlands in the north, east, and southeast. In the west, the CPR is bounded by the Eastern Alps, whereas in the south, by the Dinaridic belt.

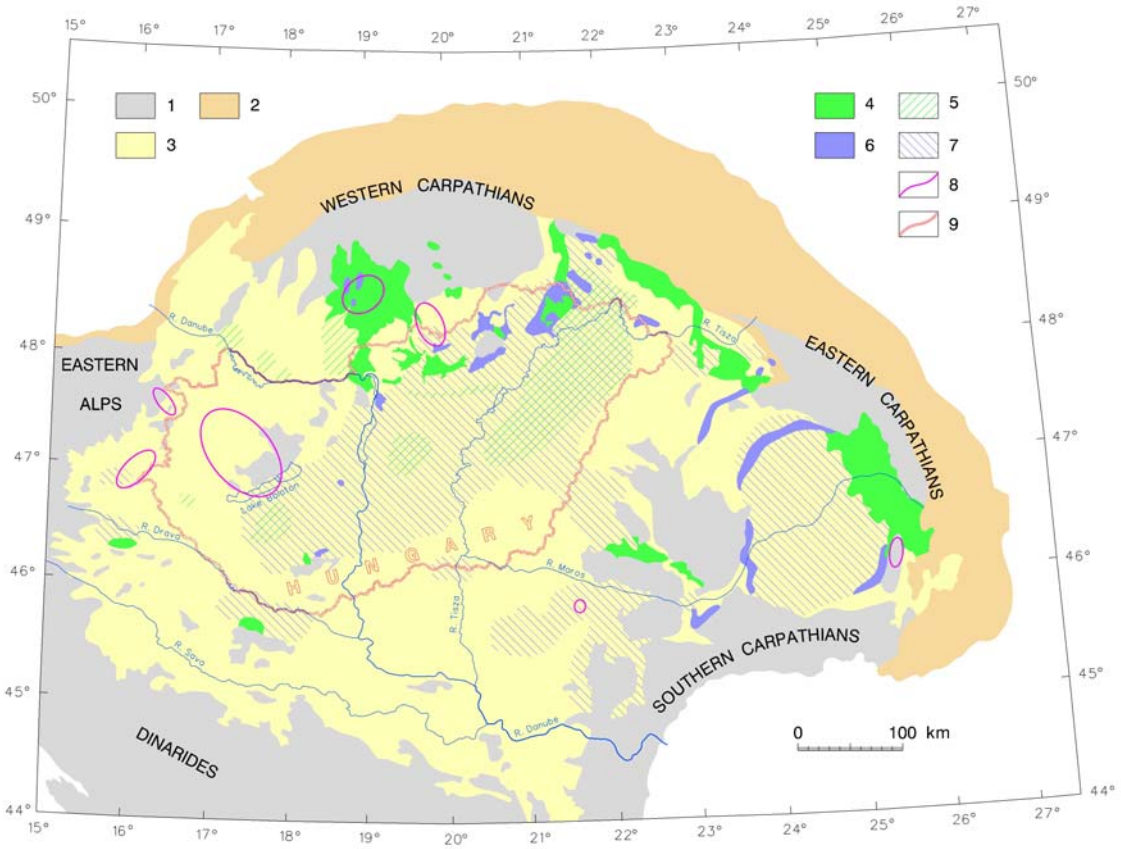

Figure 1. Map of distribution of the Neogene-Quaternary volcanic formations in the Carpatho-Pannonian Region (modified after Pécskay and others, 1995): 1 Outcrops of pre-Tertiary basement, 2 Alpine-Carpathian flysch belt, 3 Neogene-Quaternary sedimentary infill of the Pannonian Basin, 4 Outcropping intermediate volcanic rocks, 5 Buried intermediate volcanic rocks, 6 Outcropping silicic volcanic rocks, 7 Buried silicic volcanic rocks, 8 Areas of basaltic volcanism, 9 State border of Hungary.

The Cenozoic evolution of the CPR was largely governed by vigorous movements and deformations of two continental plate fragments, the Alcapa and Tisza-Dacia blocks (Csontos, 1995), that were squeezed and "milled" between the converging and colliding African and European plates. Detailed tectonic studies (*e.g.* Balla, 1980, 1981, 1987, Csontos and others, 1991, Horváth, 1993, Tari and others, 1993, 1999, Csontos, 1995, Csontos and Nagymarosy, 1998) showed that these microplates, now forming the basement of the CPR, were forced to undergo major displacements, rotations, block-faulting, tilting, and thrusting during the prevailing compressional tectonic regime, whereas at their edges subduction processes took place. Subsequently, extensional tectonics that started at 17.5 Myr B.P. (Early Miocene) presumably as a consequence of subduction roll-back and/or gravitational collapse (Csontos, 1995, Tari

and others, 1999), led to considerable lithospheric thinning, incipient rifting, and formation of large basins filled by thick sedimentary sequences up to 7000 m. As a result of an overall subsidence, these depressions, separated by elevated blocks, were united about 15 Myr ago (Middle Miocene) to form the Pannonian Basin (Hámor, 2001). There were also periods of alternating or coeval compressive-extensional regime, when shortening and attenuation, giving rise to basin subsidence and inversion, occurred simultaneously (Csontos, 1995). Major movements and brittle deformations ceased for the most part ca. 5.2 Myr ago (by the end of the Miocene) due to consolidation of the lithospheric plate motions in the region (Csontos and others, 1991, Gerner and others, 1999).

These geodynamic events were accompanied by episodic but significant magmatic activity both at the peripheries and in the interiors of the Alcapa and Tisza-Dacia microplates. In the Eocene, large andesitic stratovolcanic complexes were formed at three localities in a narrow belt (Csillag and others, 1983) to the north of what is now the Mid-Hungarian fault zone, identified as the boundary of the two microplates (Csontos, 1995, Csontos and Nagymarosy, 1998). Silicic explosive volcanism with rhyolitic (often ignimbritic), and locally dacitic tuffs, and subordinate lava flows occurred in three stages from the Early to Middle Miocene (*e.g.* Pécskay and others, 1995, Hámor, 2001). Products of the first stage also seem to be confined to the Mid-Hungarian line (Csontos, 1995), whereas the middle tuff horizon (second stage) is found throughout the Pannonian Basin, with thicknesses varying from a few meters to several hundreds of meters (Pécskay and others, 1995). Volcanites of the third stage are exposed mainly in and around NE Hungary, but minor occurrences are found throughout the region (Pécskay and others, 1995, Hámor, 2001).

From the Middle Miocene to the Pleistocene, voluminous, mostly intermediate, calc-alkaline volcanism occurred in the northern and eastern parts of the region (*e.g.* Szabó and others, 1992, Pécskay and others, 1995). The andesitic lavas and tuffs formed large, isolated stratovolcanic complexes broadly scattered in the northern part of the CPR, and a more or less continuous volcanic chain extending over 400 km in a narrow zone in the Eastern Carpathians. Moreover, commensurate with the above masses andesitic sequences are buried beneath the thick sedimentary cover in the NE part of the Pannonian Basin (Székyné Fux and Kozák, 1984), and sporadic occurrences are known from its southern part (Pécskay and others, 1995, Harangi, 2001).

Alkali basaltic lavas and tuffs erupted from the Late Miocene to the Pleistocene in several localities within the CPR (Embey-Isztin and others, 1993, Pécskay and others, 1995). These rocks form small-volume monogenetic edifices like maars, tuff-rings, lava-cones, and shield volcanoes. The largest volcanic field, with ca. 70 eruption centers, is in western Hungary, north of Lake Balaton. Other fields are situated in the western, northern, and southeastern parts of the Pannonian Basin.

There is no general consensus about the origin of these volcanic rock suites. Earlier, “classic” models regarded the above mentioned evolved rocks, including the less studied Eocene andesites, and frequently also the silicic tuffs and associated lavas, as surface manifestations of subduction processes (Pantó, 1981, Csillag and others, 1983, Salters and others, 1988, Szabó and others, 1992, Downes and others, 1995), whereas the alkaline series was generally related to lithospheric extension (Embey-Isztin and others, 1993, Szabó and others, 1992). Other studies, however, argue that only those calc-alkaline rocks erupted at the eastern periphery of the CPR are unequivocally of subduction-related origin (Póka, 1988, Harangi, 2001). The other intermediate calc-alkaline volcanites (from the northern and southern parts of the CPR), and the silicic suites are now considered to be related to lithospheric stretching (Harangi, 2001), whereas the genesis of alkaline rocks is attributed to post-extensional processes (Embey-Isztin and Dobosi, 1995, Harangi, 2001).

Besides geodynamic relationships, fundamental aspects of melt generation and magma evolution are also debated. For the silicic rocks, *e.g.*, two contrasting hypotheses have been suggested. The first is based on partial melting of the lower or upper crust (Pantó, 1981, Póka, 1988, Póka and others, 1998), whereas the second concept involves mantle-derived primary magmas modified by crustal assimilation and fractional crystallization processes (Downes and others, 1995, Harangi, 2001). In addition, locally the picture might have been further complicated by magma mixing (Póka and others, 1998, Harangi, 2001). Another example is the origin of the alkali basalts that has traditionally been explained by decompression melting in the asthenospheric mantle in response to plume arrival, with minor or no participation of the overlying lithospheric mantle (Embey-Isztin and others, 1993, Embey-Isztin and Dobosi, 1995, Harangi, 2001). However, a recent reinterpretation of the geochemical data has led to the conclusion that both the

asthenosphere and the subcontinental mantle lithosphere underwent partial melting, at least in western Hungary, giving rise to two distinct subtypes of alkali basalts with subtle but diagnostic differences in their chemical and other properties (Kovács and Ó.Kovács, in prep.).

The present study is confined to an extensive major element database of Cenozoic volcanites of Hungary (Ó.Kovács and Kovács, 2001). Nevertheless, this dataset ensures a fairly good representativeness of the volcanic formations of the whole region, as all rock types mentioned above are exposed in Hungary, except for the subduction-related calc-alkaline andesitic series of the Eastern Carpathians. Thus, a geomathematical analysis of these data may expectedly contribute to the understanding of petrogenetic processes that occurred in the CPR during the Cenozoic. More specifically, the aim of this work is to understand the major element compositional variation of the studied volcanic complexes, based on a large number of samples, through establishing the principal compositional trends within these sets, and attempting to reveal or reject any possible link between the trends.

2 Main features of the database

A detailed description of the database used in the present paper is given in Ó.Kovács and Kovács (2001), therefore here only a few main characteristics are provided. Three types of data sources were used in data collection: (1) comprehensive studies on the three major volcanic areas of Hungary, those of the Mátra Mts., Tokaj Mts. and Börzsöny Mts., and all other relevant publications, (2) a great number of technical reports of different scope and objective, and (3) several existing specialized databases after inevitable revision and modification. As a result, data of well over 3000 samples of Cenozoic volcanites with major element chemistry were collected. Only individual samples were selected, *i.e.* average compositions were not considered.

Reliability of numerical data is always important in a computerized environment. The collected data are rather heterogeneous regarding both the place and time of chemical analyses performed; *i.e.* different laboratories, analysts and, partly, methods have been involved. The dates of analyses roughly span the twentieth century. Luckily, all these analytical data have a common feature, namely, the expected sum of major oxides expressed in weight % should be close to 100. Only samples satisfactorily approximating this expectation were incorporated, and analytical error-related anomalies were tried to be eliminated.

For simplicity, the data are organized into one table (created in "dbf"-format). Each row (record) of the table represents an analyzed rock sample; columns (fields) correspond to attributes of samples. The attributes form several groups: a complete reference of all data sources, the most possible exact location of each sample, ages and lithostratigraphic units of the rocks analyzed, original major element and related chemical data, component values recalculated on a common basis, and some relevant background information.

The list of major components analyzed and used in different publications is not always standard, which is especially true for earlier sources; *e.g.*, components like SO_3, Ba, Sr, S, or Cl, are rarely present. Although they are all included in the database, the basic set of components comprises the most widely used major oxides: SiO_2, TiO_2, Al_2O_3, Fe_2O_3, FeO, MnO, MgO, CaO, Na_2O, K_2O, P_2O_5, H_2O^+, H_2O^-, and CO_2. Even some of these components are not given in all sources, and in a number of samples they may have "values below detection limit", frequently recorded as 0.00%, which is neither possible (in principle) nor favorable for statistics. All this information is maintained in the database. Mainly in earlier analyses, for Fe total-iron is given (also not in a standard form, *i.e.* either as Fe_2O_3 or as FeO); therefore (a uniform) total-iron has been calculated in each case, and is considered a basic component when Fe^{2+} and Fe^{3+} are not determined.

3 Pre-treatment of data

As the set of major components determined has not been absolutely standard, even the good-quality analyses are not directly comparable. The problem of iron can be circumvented, to a certain extent, by computing total iron expressed in a unique form (here as $Fe_2O_3^{total}$) for all samples (see above), but this also means loosing part of the available information, namely the relative abundance of Fe^{2+} and Fe^{3+}. Similar, but a little more complex, is the problem of volatile components. The final common denominator

might be loss-on-ignition (LOI), although the ignition procedure is not standardized among laboratories. But even LOI is not unambiguous, as sometimes H_2O^- — water released on heating up to 105 (or 110) °C — is included. Furthermore, in the literature, unfortunately, H_2O^- is often used as a regular component in spite of the fact that it is nothing else but the dampness of the sample. In this study, in order to make accessible for statistics as many samples as possible, all analyses were recalculated also on a LOI-free (*i.e.* volatiles-free) basis, thus assuring comparability of the other major components.

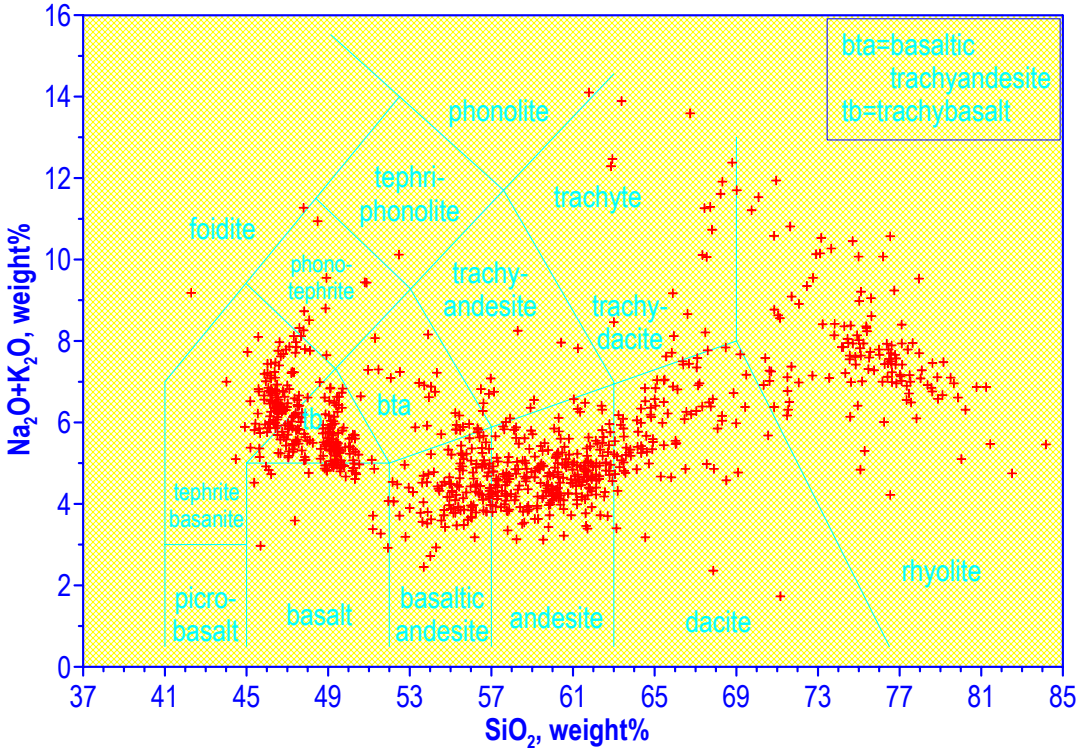

Figure 2. TAS-diagram, as suggested by Le Bas and others (1986), of 964 fresh rock samples from the Cenozoic volcanites of Hungary. Selected samples satisfy: $H_2O<2\%$, $CO_2<0.5\%$, and LOI<3%.

In recognizing/resolving many geologic problems, individual observations with anomalous values in one or several components are very informative. However, the statistical behavior of a sample is often distorted or obscured by them. Different applications may require different conditions to rely on. For example, a widely used volcanic rock naming scheme suggested by Le Maitre (1984) and later adjusted by Le Bas and others (1986) only allows unaltered rock samples to be used (Fig. 2), which are considered to have $H_2O<2\%$, $CO_2<0.5\%$, and LOI<3%. In this work, general statistical features of entire volcanic complexes are searched for; hence only samples with the most extreme values are excluded from the analysis. The applied upper threshold corresponds to the 99th percentile for each component, corrected by some petrochemical considerations. As a result, 2260 samples were submitted to statistical investigation. Therefore, a direct comparison with the mentioned fresh rock samples (Fig. 2) is not possible, and is left for a future study.

4 Statistical analysis

The TAS diagram is a somewhat standard representation of the type of data selected for our analysis (Fig. 2). It has been used for years with useful results, *e.g.* to evidence patterns like the one shown in Figure 2, which might be an indication of petrogenetic processes undergone by the parental magmas. Our purpose is to model and improve interpretation of such processes using a statistical analysis based on the assumption that relative differences between observed values are more meaningful than absolute ones.

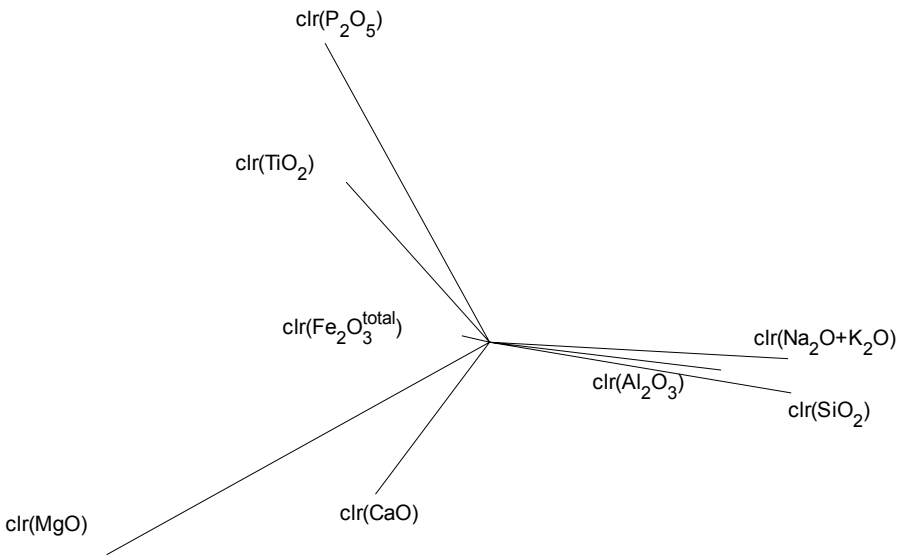

Figure 3. Biplot in the clr-transformed space.

In order to retain a link to the TAS diagram, in our analysis we use the amalgamated component Na_2O+K_2O. The compositional biplot (Aitchison and Greenacre, 2002) of the resulting set of eight components — (SiO_2, TiO_2, Al_2O_3, $Fe_2O_3^{total}$, MgO, CaO, Na_2O+K_2O, P_2O_5) — is shown in Figure 3. Recall that the compositional biplot is a standard biplot computed on the centered logratio (clr) transformed parts of a composition. The centered logratio transformation (Aitchison, 1986) is defined as an application going from the D-part simplex to D-dimensional real space R^D. It consists of computing the geometric mean g_i of each sample, dividing each component x_{ij} in the i-th sample by it, and finally taking the natural logarithm. Thus, for each i=1, 2, …, n, where n is the number of samples, we compute:

$$\mathrm{clr}(x_{i1}, x_{i2},\ldots, x_{iD}) = (\ln(x_{i1}/g_i), \ln(x_{i2}/g_i),\ldots, \ln(x_{iD}/g_i)),$$

and we denote each component in the image space simply by $\mathrm{clr}(x_j)$, as shown in Figure 3.

Table 1. Variation matrix. (Lower triangle: $E[\ln(x_i/x_j)]$ || Upper triangle: $\mathrm{Var}[\ln(x_i/x_j)]$)

x_j || x_i	SiO_2	TiO_2	Al_2O_3	$Fe_2O_3^{total}$	MgO	CaO	Na_2O+K_2O	P_2O_5
SiO_2	*	1.0558	0.3248	0.8545	1.3685	0.9964	0.4908	1.1585
TiO_2	4.5452	*	0.9089	0.6649	0.9991	0.8925	1.0558	0.7627
Al_2O_3	1.2915	-3.2537	*	0.6887	1.2676	0.8857	0.5016	1.0533
$Fe_2O_3^{total}$	2.4386	-2.1066	1.1471	*	1.0013	0.7392	0.8721	0.8933
MgO	3.4304	-1.1148	2.1389	0.9918	*	0.9052	1.3899	1.1213
CaO	2.5564	-1.9888	1.2649	0.1177	-0.874	*	1.0208	0.9927
Na_2O+K_2O	2.525	-2.0202	1.2335	0.0864	-0.9054	-0.0314	*	1.1373
P_2O_5	5.9909	1.4458	4.6995	3.5523	2.5606	3.4346	3.466	*

The biplot has, among others, the following characteristics:

(a) Each ray shown in a biplot is associated to one clr-transformed variable $\mathrm{clr}(x_i)$. The endpoint of each ray is called a vertex.

(b) If the proportion of total variability explained by a biplot is reasonably high, then the length of each ray is roughly proportional to the variance of that clr-transformed component and the link between the vertices of two rays is roughly proportional to the variance of $\ln(x_i/x_j)$; the numerical values of these variances can be seen in the upper triangle of the variation matrix in Table 1.

(c) If two vertices are very close together, then the value of $\mathrm{var}(\ln(x_i/x_j))$ is approximately zero, what might indicate that x_i and x_j are roughly proportional.

(d) If three or more vertices are on a straight line, it might indicate a one-dimensional variability between the parts. For three vertices it appears as a trend in the ternary diagram of the corresponding parts. The trend is linear in the usual sense whenever two vertices of the three are close together, and curved

if the three vertices lie apart. In both cases they are lines with respect to the geometry of the simplex, which we call compositional lines (Aitchison and others, 2002).

For a detailed account on the characteristics and properties of this powerful tool, see Aitchison (2001) and Aitchison and Greenacre (2001). For a summary and/or applications in the field of geosciences, see Aitchison (1990), Pawlowsky-Glahn and Buccianti (2002), Buccianti and Pawlowsky-Glahn (2002), von Eynatten and others (2003a, 2003b) and Martín-Fernández and others (2003).

Consider now the biplot in Figure 3. The proportion of total variability explained is 69.94%, which is just on the border between reasonably high and too low. Therefore, indications have to be taken with care.

As can be observed, the ray corresponding to clr($Fe_2O_3^{total}$) is extremely short — which might indicate that, in each sample, $Fe_2O_3^{total}$ is roughly proportional to the geometric mean of the components of sample — whereas the rays of clr(MgO), clr(P_2O_5), clr(SiO_2) and clr(Na_2O+K_2O) are the largest. Thus, to obtain a ternary plot with probably large dispersion, we would use the parts MgO and P_2O_5 with either SiO_2 or Na_2O+K_2O, which will be quite similar due to the fact that the vertices clr(SiO_2) and clr(Na_2O+K_2O) lie close together. Note that in Table 1 the variance of ln(SiO_2/Na_2O+K_2O) is pretty small (0.4908), while var(ln(SiO_2/MgO))=1.3685, var(ln(MgO/Na_2O+K_2O))=1.3899, and for the third component we obtain the values var(ln(SiO_2/P_2O_5))=1.1585, var(ln(Na_2O+K_2O/P_2O_5))=1.1373, and var(ln(MgO/P_2O_5))= 1.1213. Figures 4A and 4B display the subcomposition in a ternary diagram with and without centering. The centering operation was first introduced by Martín-Fernández and others (1999), and was extensively studied as a tool for geological data visualization by von Eynatten and others (2002). Other publications in which it is used for representing geological data are Buccianti and others (1999), Pawlowsky-Glahn and Buccianti (2002) and von Eynatten and others (2003b). Despite that in the non-centered representation in Figure 4A the pattern of the data might look like a linear trend in the usual Euclidean sense, after centering we see an extremely large dispersion in the data, no clear trend, and only two relatively important accumulations of samples. They indicate actually the presence of two populations (Fig. 4B) corresponding to basaltic and calc-alkaline rock samples, as shall be seen later. Recall that the metric considered is relative, and not absolute, which implies that samples close to the border of the triangle are considered to be very different.

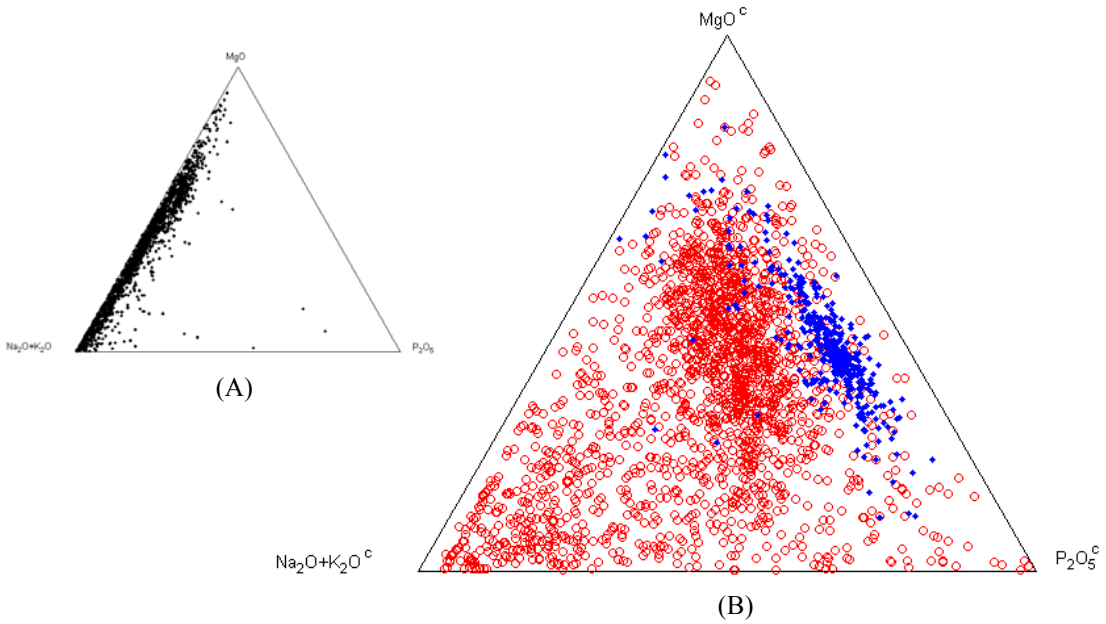

Figure 4. (MgO, Na_2O+K_2O, P_2O_5) subcomposition: (A) not centered; (B) centered. Red circles stand for calc-alkaline rocks, blue diamonds for basaltic rocks. Superindex ^{c} in (B) indicates centered parts.

Consider now the position of the vertices clr(SiO_2), clr(Al_2O_3) and clr(Na_2O+K_2O) in the biplot (Fig. 3). They are pretty close in the diagram, the corresponding variances in the variation matrix are effectively the smallest, and a ternary diagram of the three parts will probably show little variability. At the same time, the ternary diagrams including any two of them, but particularly SiO_2 and Na_2O+K_2O, and a third component whose vertex lies farther apart, will probably show a linear trend in the usual sense, as can be seen in Figures 5A and 5B taking as third part MgO. Two curved trends would be probably evidenced as well if the ternary diagrams associated to (P_2O_5, TiO_2, CaO) or (MgO, CaO, SiO_2) are plotted, given that the corresponding vertices are roughly aligned.

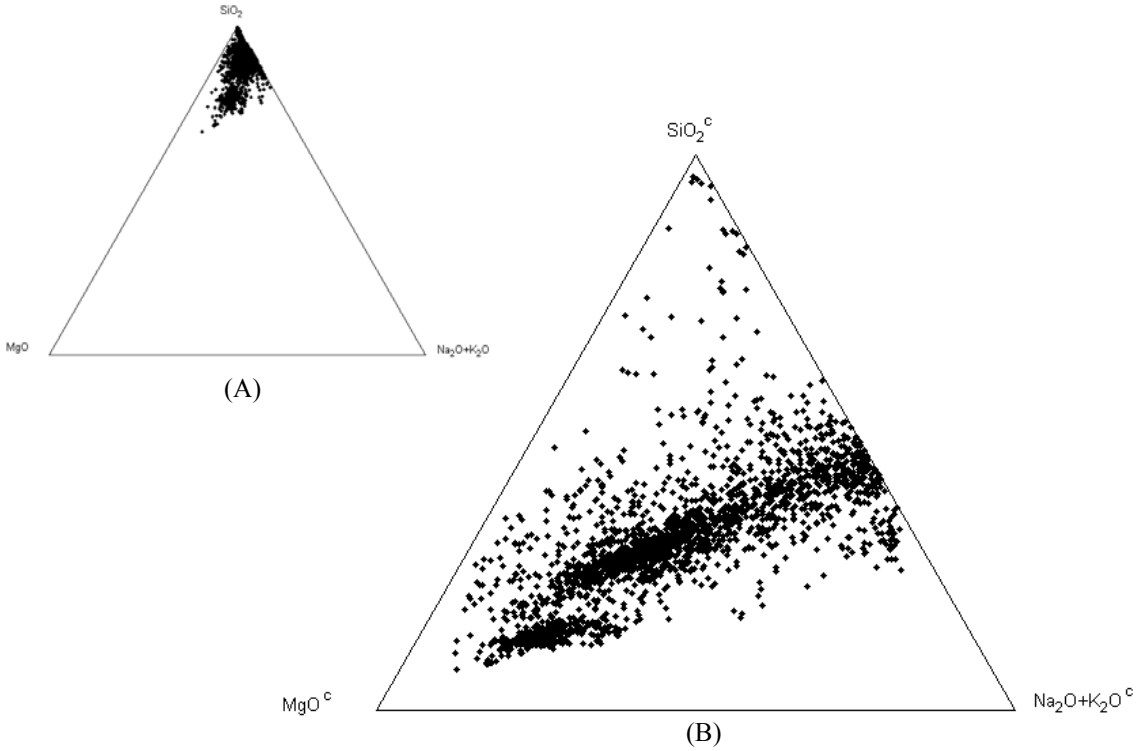

Figure 5. (SiO_2, MgO, Na_2O+K_2O) subcomposition: (A) not centered; (B) centered. Superindex ^{c} in (B) indicates centered parts.

A closer look at Figure 5B shows the clear presence of two roughly linear compositional trends associated to the basaltic rocks, and the calc-alkaline series, which have been distinguished by different symbols in Figure 6. The two trends have been modeled using compositional principal component analysis (Aitchison, 1986; Aitchison and Thomas, 1998; Pawlowsky-Glahn and Buccianti, 2002b; von Eynatten and others, 2003b) on each of the two groups, leading to a direction vector (0.3287;0.1334;0.5379) for basalts, with a compositional center given by (0.7859; 0.1216; 0.0926) and 78.47% variability of the subcomposition explained. In the case of the calc-alkaline suite the corresponding values are (0.4059; 0.1285; 0.4656) for the direction vector, (0.9122; 0.0208; 0.0670) for the compositional center and 91.23% for the explained variability. The two trends have been plotted both non-centered (Fig. 6A) and centered (Fig. 6B). Observe that the two compositional lines have an intersection point close to the MgO^c vertex in Figure 6B and between the MgO and the SiO_2 vertex in Figure 6A. This intersection point has been computed as (0.5418; 0.4321; 0.0260) and represented with the trends and the data in Figure 6A.

A possible reading of the model obtained is the following: assume the intersection point represents the mean composition of a parental magma for both types of rocks. Thus, if we consider only the sub-composition (SiO_2, MgO, Na_2O+K_2O), the parental magma would present a composition varying around the point (0.5418; 0.4321; 0.0260), which turns into less variable basalts, centered at (0.7859; 0.1216; 0.0926), through a perturbation process defined by the direction vector (0.3287; 0.1334; 0.5379). The same parental magma would turn into highly variable calc-alkaline rocks, centered at (0.9122; 0.0208; 0.0670), through a perturbation process defined by the direction vector (0.4059; 0.1285; 0.4656). This can be written for the basalts as

$(SiO_2(t), MgO(t), Na_2O+K_2O(t)) = C[(0.5418 \times 0.3287^t; 0.4321 \times 0.1334^t; 0.0260 \times 0.5379^t)]$,

and for the calc-alkaline suite as

$(SiO_2(t), MgO(t), Na_2O+K_2O(t)) = C[(0.5418 \times 0.4059^t; 0.4321 \times 0.1285^t; 0.0260 \times 0.4656^t)]$,

where C stands for the closure operation:

$$C[(x_1, x_2, ..., x_D)] = \left(\frac{100\, x_1}{\sum x_k}, \frac{100\, x_2}{\sum x_k}, ..., \frac{100\, x_D}{\sum x_k} \right).$$

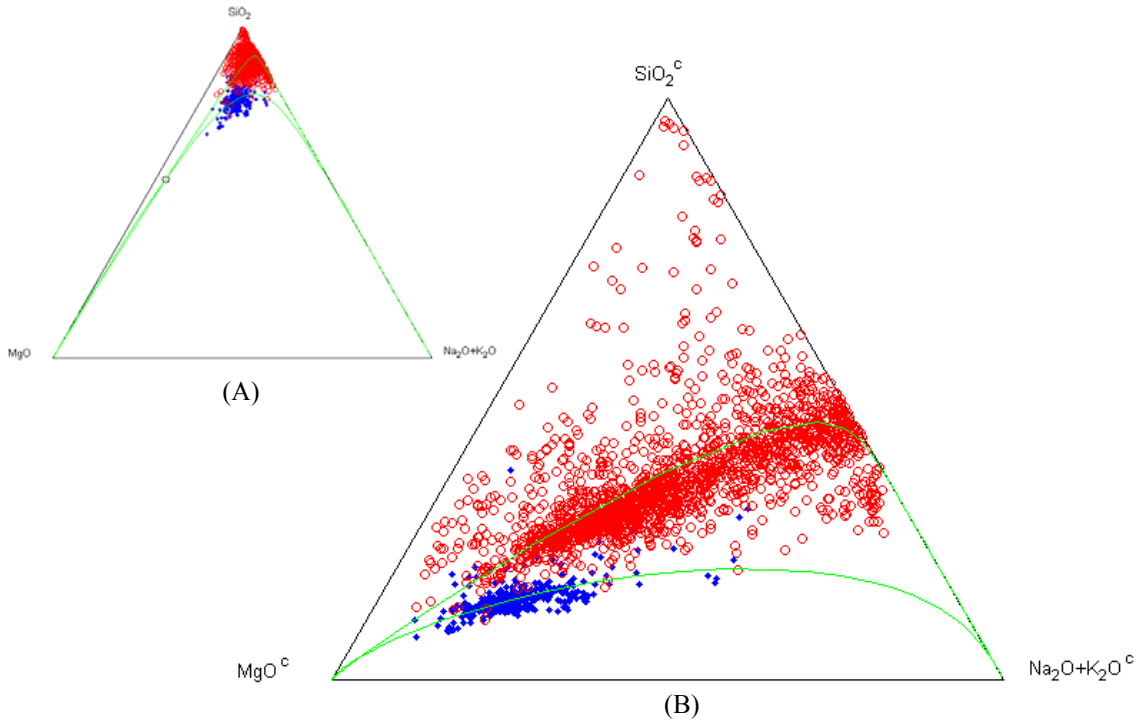

Figure 6. (SiO_2, MgO, Na_2O+K_2O) subcomposition: (A) not centered; (B) centered. Red circles represent calc-alkaline rocks; blue diamonds basaltic rocks. Green lines show the first principal axe of each group. Superindex ^{c} in (B) indicates centered parts.

The basaltic rocks reach the center at t=1.8189, while the calc-alkaline series does it for t=3.0903. The value of t can be regarded as an index of magma evolution. Figures 7A and 7B show the intersection point, with numbered tics on the two trends indicating the values of t required to reach the marked points.

Finally, we attempt to represent approximately the trends obtained in the TAS-diagram in order to illustrate the differences between basaltic and calc-alkaline data in a familiar representation. To be able to do so, we use the fact that the D-part simplex is a Euclidean space with operations fully compatible with centering and relative differences (Aitchison and others, 2002). This fact has enabled us to use the concept of orthonormal basis associated to a composition which is subcompositionally coherent (Egozcue and others, 2003), and to combine the determination of the trends shown in Figures 7A and 7B in the 3-part simplex defined by the subcomposition (SiO_2, MgO, Na_2O+K_2O) with regression analysis. The result, shown in Figure 8, is a reasonable approximation, but is not completely satisfactory. The trends shown in Figure 7A and 7B are obtained using principal component analysis in a two dimensional space and correspond to the first principal component of two. In Figure 8, the first principal component captures reasonably well the pattern of the calc-alkaline suite, but not the pattern of the basaltic rocks, which is much better represented by the second principal component. This result is in part not surprising, as the trends in Figures 7A and 7B reflect essentially the relative variability of MgO. It makes clear that further study is required to see if there is a way to model the pattern observed in the classical TAS diagram using compositional geometry as introduced by Aitchison (1986) and further developed in Aitchison and others (2002), or if alternative diagrams are required to show it. Interesting should be also

modeling of the trends obtained in the light of the differential perturbation models discussed in Aitchison and Thomas (1998).

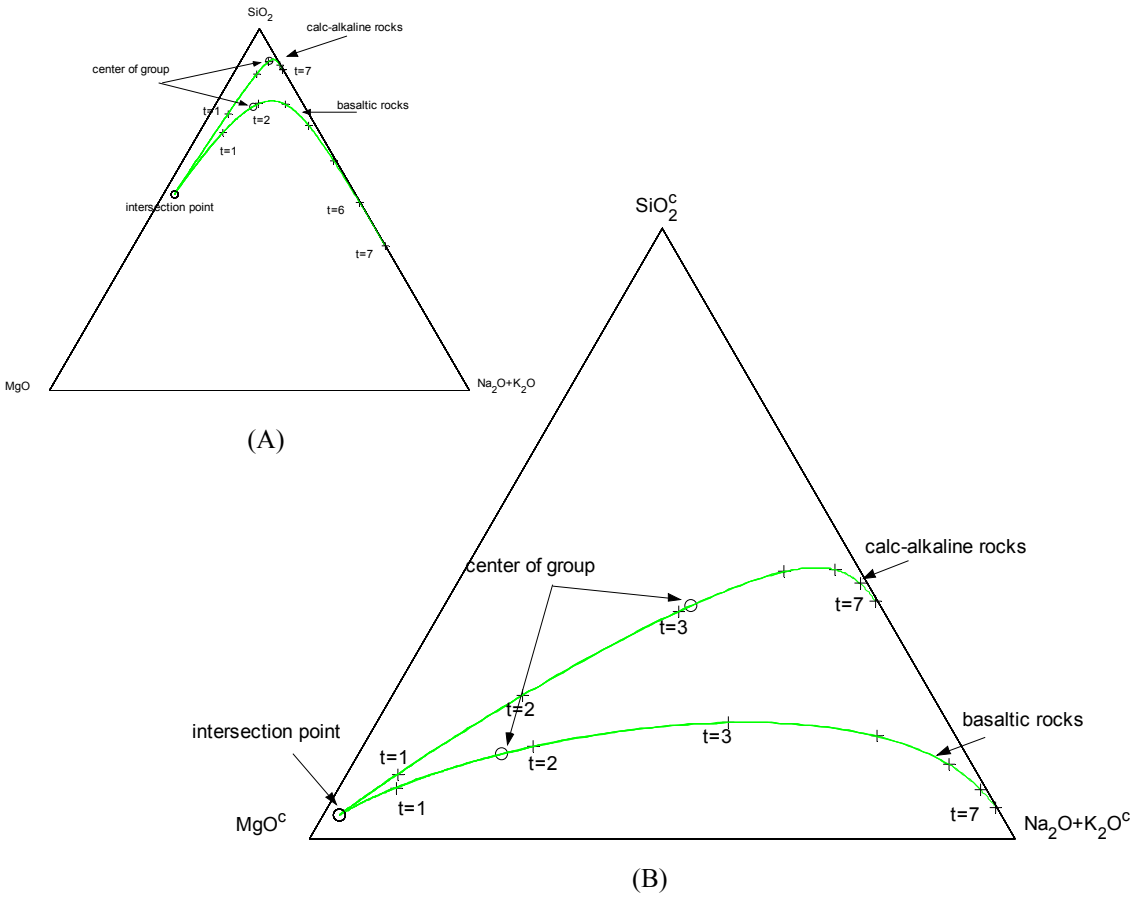

Figure 7. Trends (green lines) associated to calc-alkaline and basaltic rocks for (SiO_2, Na_2O+K_2O, MgO): (A) not centered; (B) centered. Superindex ^{c} in (B) indicates centered parts.

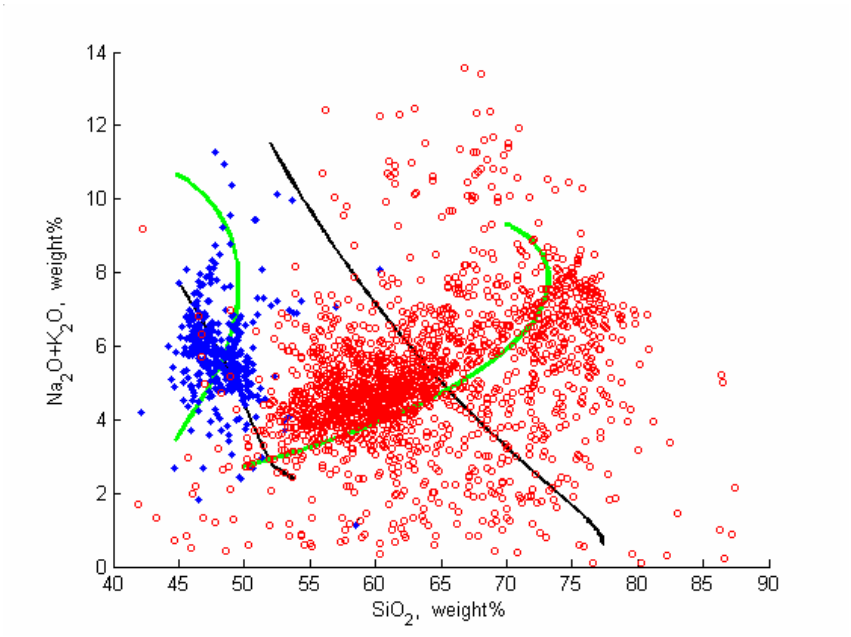

Figure 8. TAS-diagram showing calc-alkaline (red circles) and basaltic rocks (blue diamonds). Green lines correspond to the first principal axes of each group, black lines to the second principal axes.

5 Geologic interpretation

The existence of well-defined compositional trends is consistent with the general understanding of magma evolution. The two different trends established through the statistical analysis may help to distinguish between the petrogenetic concepts outlined in the Introduction.

The revealed trends reflect ordinary processes of progressive magma differentiation, though apparently diverse processes for the two rock groups. For the basaltic rocks, crystal fractionation, *i.e.* crystallization and successive settling out of high-Mg minerals can account for the observed linear trend (78.47% explained variability). Detailed geochemical studies (*e.g.* Embey-Isztin and others, 1993) showed that other differentiation processes which could cause major shift in magma composition (*e.g.* modification due to assimilation of crustal material *en route* to the surface) did not influence the basalts of the region.

In contrast, the neat trend fit by the calc-alkaline rocks (andesites to rhyolites; 91.23% explained variability) could unlikely be explained by fractional crystallization alone. Rather, it is a combined outcome of more than one process affecting the magma composition. Though, in principle, both intermediate (andesitic) and silicic (dacitic to rhyolitic) rocks may derive by crystal fractionation from more primitive (*e.g.* basaltic, or andesitobasaltic) magmas, the huge amounts of such volcanites (locally forming piles up to several 1000 meters thick) in the region rule out this process as the dominant one in their petrogenesis. Instead, we suggest that the evolutionary trend gained for all these (calc-alkaline) rocks reflects, in the first place, mixing between two distinct end-member magma types. Mantle-derived andesitic magmas from one side, and rhyolitic magmas produced by direct partial melting of the crust from the other, could serve as the end-members. Presence of volcanic rocks with such „extreme" compositions in the region has been inferred from trace element and isotope geochemical data (*e.g.* Downes and others, 1995, Póka and others, 1998, Harangi, 2001). It is also worth noting that fitting one general trend by essentially all the investigated calc-alkaline rock samples is a major, and far not obvious feature that emphasizes their genetic closeness.

Table 2. Compositions of the intersection point and assumed mantle

	SiO_2	**MgO**	**Na_2O+K_2O**	**SiO_2 : MgO**	**Reference**
	weight %				
Intersection point	54.18	43.21	2.60	55.63 : 44.37	this work
Assumed mantle composition	45.96	37.78	0.36	54.88 : 45.12	Hart and Zindler, 1986
	44.76	37.23	0.64	54.59 : 45.41	Ringwood, 1991
	45.00	37.80	0.39	54.35 : 45.65	McDonough and Sun, 1995
	46.12	37.77	0.39	54.98 : 45.02	Allègre and others, 1995

The fact that these two compositional trends converge, and intersect at high MgO contents may be of particular importance. The intersection point may hint to a very primitive magma composition that was a common parent for the two rock suites. In Table 2, the values of three principal oxides are compared to those given for estimated mantle composition by several authors. The similarity of the SiO_2 : MgO ratio in the intersection point with that in the assumed mantle is amazing and thought to be convincing. (We note that the slight differences in the MgO and SiO_2 contents, and the more remarkable difference in total alkalis between the mantle estimations and the intersection point are fully consistent with the behavior of these elements: during melting of the mantle, Na and K, and to a lesser extent Si, tend to partition into the melt rather than to remain in the mantle minerals, whereas the opposite is true for Mg.) Therefore, this finding may further corroborate earlier inferences that some of the parental magmas of the calc-alkaline suite may have had a mantle source similar or identical to that of the basalts (*e.g.* Salters and others, 1988, Downes and others, 1995).

The unsatisfactory fitting of trend lines to the basaltic rocks on the TAS diagram (Fig. 8) may be due to the presence of two subgroups within this rock suite (Kovács and Ó.Kovács, in prep.). A compositional data analysis considering the basaltic suite alone could expectedly provide a better resolution in revealing compositional variations for these rocks. Similarly, a closer look at the silicic rocks separately could certainly distinguish a "subtrend" for the K-metasomatized volcanites forming a small subgroup in the high Na_2O+K_2O field, *e.g.* in Figure 4B, 5B and 8. These geochemically altered rocks merge into the

general calc-alkaline trend when all data are analyzed together, due to their low MgO, high SiO_2, and extremely high alkali contents.

6 Conclusions

So far, few geoscience case studies can be found in the literature that make extensive use of statistical methods based on the compositional geometry and the assumption that relative differences are more significant for percentage data than absolute differences. Nevertheless, its use shows once and again a surprisingly good agreement with geological models based on scientific methods which do not include a statistical approach. Such is the case of the estimated composition of the parental magma for the subcomposition (SiO_2, MgO, Na_2O+K_2O). It is obtained as the intersection of two principal components associated one to the basaltic rocks, the other to the calc-alkaline rocks.

The combination of compositional principal component analysis within a subspace, with regression analysis within the whole simplex, used to obtain an approximate representation of the trends obtained in the TAS diagram is only possible considering the simplex as a Euclidean space. This first attempt gives reasonable results and opens up a door to deeper studies in this direction.

The suggested geologic interpretation is a very general understanding of certain statistical features of the data. Although it is consistent with the prevailing ideas about the geologic history of the region, it certainly needs further refinement. For this, similar geologic applications suitable for comparison would be needed, and, in order to gain important details for the evolution of the involved magmas, appropriately selected subsets of the observations should be statistically analyzed.

Acknowledgements

This paper was created in the frame of the Hungarian-Spanish Intergovernmental Scientific and Technological Co-operation (Project number: E-6/2001), approved by the 9th Joined Commission.

References

Aitchison, J., 1986, The statistical analysis of compositional data: Chapman and Hall, London, 416 p.

Aitchison, J., 1990, Relative variation diagrams for describing patterns of compositional variability: Mathematical Geology, 22, p. 487-511.

Aitchison, J., 2001, Simplicial inference. — In: Algebraic Methods in Statistics (eds. M. Viana and D. Richards), Contemporary Series of the American Mathematical Society.

Aitchison, J., and Greenacre, M., 2002, Biplots of compositional data: Applied Statistics, 51, p. 375-392.

Aitchison, J., and Thomas, C. W., 1998, Differential perturbation processes: a tool for the study of compositional processes, in Buccianti A., Nardi, G. and Potenza, R., eds., Proceedings of IAMG'98 - The Fourth Annual Conference of the International Association for Mathematical Geology: De Frede Editore, Napoli (I), p. 499-504.

Aitchison, J., Barceló-Vidal, C., Egozcue, J.J. and Pawlowsky-Glahn, V., 2002, A concise guide for the algebraic-geometric structure of the simplex, the sample space for compositional data analysis. — In: Burger, H. and Skala, W. (eds.) Proceedings of IAMG'02, The 8th Annual Meeting of the International Association for Mathematical Geology, 15-20 September 2002, Berlin, Germany, p. 387-392.

Allègre, C.J., Poirier, J.P., Humler, E., and Hofmann, A.W., 1995, The chemical composition of the Earth: Earth Planet Sci. Lett., 134, p. 515-526.

Balla, Z., 1980, Neogene volcanites in the geodynamic reconstruction of the Carpathian region: Geophys. Trans., 26, p. 5-43.

Balla, Z., 1981, Neogene volcanism of the Carpatho-Pannonian region: Earth Evol. Scien., 3-4, p. 240-248.

Balla, Z., 1987, Tertiary paleomagnetic data for the Carpatho-Pannonian region in the light of Miocene rotation kinematics: Tectonophysics, 139, p. 67-98.

Buccianti, A., Pawlowsky-Glahn, V., Barceló-Vidal, C. and Jarauta-Bragulat, E., 1999, Visualization and modeling of natural trends in ternary diagrams: a geochemical case study. — In: Lippard, S. J., Naess, A. and Sinding-Larsen, R. (eds), Proceedings of IAMG'99, The Fifth Annual Conference of the International Association for Mathematical Geology, Vol. 1, Tapir, Trondheim (N), p. 139-144.

Buccianti A. and Pawlowsky-Glahn V., 2002, Random variables and geochemical processes: a way to describe natural processes. — In: Special volume on National Geochemical Mapping. Project sponsored by SoGeI (Italian Geochemical Society), ANPA (National Environmental Protection Agency) and CNR (National Research Council).

Csillag, J., Földessy, J., Zelenka T., and Balázs, E., 1983, The plate tectonic setting of the Eocene volcanic belt in the Carpathian Basin. – In: Bisztricsány, E., and Szeidovitz, Gy. (eds): Proc., 17th Assembly, European Seismological Commission, Budapest, p. 589-599.

Csontos, L., 1995, Tertiary tectonic evolution of the Intra-Carpathian area: a review: Acta Vulcan., 7/2, p. 1-13.

Csontos, L., Tari, G., Bergerat, F., and Fodor, L., 1991, Evolution of the stress field in the Carpatho-Pannonian area during the Neogene: Tectonophysics, 199, p. 73-91.

Csontos, L., and Nagymarosy, A., 1998, The Mid-Hungarian line: a zone of repeated tectonic inversions: Tectonophysics, 297, p. 51-71.

Downes, H., Pantó, Gy., Póka, T., Mattey, D.P., and Greenwood, P.B., 1995, Calc-alkaline volcanics of the Inner Carpathian arc, Northern Hungary: new geochemical and oxygen isotopic results: Acta Vulcan., 7/2, p. 29-41.

Egozcue, J. J., Pawlowsky-Glahn, V., Mateu-Figueras, G. and Barceló-Vidal, C., 2003, Isometric logratio transformations for compositional data analysis, Mathematical Geology, 35, p. 279-300.

Embey-Isztin, A., Downes, H., James, D.E. Upton, B.G.J., Dobosi, G., Ingram, G.A., Harmon, R.S., and Scharbert, H.G., 1993, The petrogenesis of Pliocene alkaline volcanic rocks from the Pannonian Basin, Eastern Central Europe: J. Petrol., 34, p. 317-343.

Embey-Isztin, A., and Dobosi, G., 1995, Mantle source characteristics for Miocene-Pleistocene alkali basalts, Carpathian-Pannonian Region: a review of trace elements and isotopic composition: Acta Vulcanol., 7/2, p. 155-166.

Gerner, P., Bada, G., Dövényi, P., Müller, B., Onescu, M.C., Cloething, S., and Horváth, F., 1999, Recent tectonic stress and crustal deformation in and around the Pannonian Basin: data and models. – In: Durand, B., Jolivet, L., Horváth, F., Séranne, M. (eds): The Mediterranean Basins: Tertiary Extension within the Alpine Orogen: Geol. Soc. London, Spec. Publ., 156, p. 269-294.

Hámor G., 2001, Genesis and evolution of the Pannonian Basin. – In: Haas J. (ed.): Geology of Hungary: Eötvös Univ. Press, Budapest, p. 193-265.

Harangi, Sz., 2001, Neogene to Quaternary volcanism in the Carpathian-Pannonian Region – a review: Acta Geol. Hung., 44, p. 223-258.

Hart, S.R., and Zindler, A., 1986, In search of a bulk-earth composition: Chem. Geol.., 57, p. 247-267.

Horváth, F., 1993, Towards a mechanical model for the formation of the Pannonian basin: Tectonophysics, 225, p. 333-358.

Kovács, P.G., and Ó.Kovács, L. (in prep.), Bimodality of the Cenozoic alkali basalts in Transdanubia (western Hungary).

Le Bas, M.J., Le Maitre, R.W., Streckeisen, A., and Zanettin, B., 1986, A chemical classification of volcanic rocks based on the total alkali–silica diagram: J. Petrol., 27, 3, p. 745-750.

Le Maitre, R.W., 1984, A proposal by the IUGS Subcommission on the Systematics of Igneous Rocks for a chemical classification of volcanic rocks based on the total alkali silica (TAS) diagram: Austral. Jour. Earth Scien, 31, p. 243-255.

Martín-Fernández, J. A., Bren, M., Barceló-Vidal, C. and Pawlowsky-Glahn, V., 1999, A measure of difference for compositional data based on measures of divergence. — In: Lippard, S. J., Naess, A. and Sinding-Larsen, R. (eds), Proceedings of IAMG'99, The Fifth Annual Conference of the International Association for Mathematical geology, Vol. 1, Tapir, Trondheim (N), p. 211-216.

McDonough, W.F., and Sun, S.-S., 1995, The composition of the Earth: Chem. Geol., 120, p. 223-253.

Ó.Kovács, L., and Kovács, G.P., 2001, Petrochemical database of the Cenozoic volcanites in Hungary: structure and statistics: Acta Geol. Hun., 44, 4, p. 381-417.

Pawlowsky-Glahn, V. and Buccianti, A., 2002a, Visualization and modeling of subpopulations of compositional data: statistical methods illustrated by means of geochemical data from fumarolic fluids, International Journal of Earth Sciences (Geologische Rundschau), vol. 91, p. 357-368.

Pawlowsky-Glahn V. and Buccianti A., 2002b, The statistical analysis of compositional data: from theory to practice. — In: Buccianti, A., Marini, L., Ottonello, G., and Vaselli, O. (eds), Proceedings of the Arezzo Seminar on Fluid Geochemistry, DIPTERIS, Università di Genova, p. 61-73.

Pantó, Gy., 1981, Rare earth element geochemical pattern of the Cenozoic volcanism in Hungary: Earth Evol. Scien., 1, 3-4, p. 249-256.

Pécskay, Z, Lexa, J., Szakács, A., Balogh, K., Seghedi, I., Konečný, V., Kovács, M., Márton, E., Kaličiak, M., Széky-Fux, V., Póka, T., Gyarmati, P., Edelstein, O., Rosu, E., and Žec, B., 1995, Space and time distribution of Neogene-Quarternary volcanism in the Carpatho-Pannonian Region: Acta Vulcan., 7/2, p. 15-28.

Póka, T., 1988, Neogene and Quaternary volcanism of the Carpathian-Pannonian Region: Changes in chemical composition and its relationship to basin formation. – In: The Pannonian Basin. A study in basin evolution. AAPG Memoir, 45, p. 257-277.

Póka, T., Zelenka, T., Szakács, A., Seghedi, I., Nagy, G., and Simonits, A., 1998, Petrology and geochemistry of the Miocene acidic explosive volcanism of the Bükk Foreland, Pannonian Basin, Hungary: Acta Geol. Hung., 41, p. 437-466.

Ringwood, A.E., 1991, Phase transformations and their bearing on the constitution and dynamics of the mantle: Geochim. Cosmochim. Acta, 55, p. 2083-2110.

Salters, V.J.M, Hart, S.R., and Pantó, Gy., 1988, Origin of Late Cenozoic volcanic rocks of the Carpathian arc, Hungary. – In: The Pannonian Basin. A study in basin evolution. AAPG Mem., 45, p. 279-292.

Szabó, Cs., Harangi, Sz., and Csontos, L., 1992, Review of Neogene and Quaternary volcanism of the Carpathian-Pannonian region: Tectonophysics, 208, p. 243-256.

Székyné Fux, V., and Kozák M., 1984, A Nyírség mélyszinti neogén vulkanizmusa (Deep-situated Neogene volcanism in the Nyírség, NE Hungary.): Földt. Közl., 114, p. 149-159 (in Hungarian).

Tari, G., Báldi, T., and Báldi-Beke, M., 1993, Paleogene retroarc flexural basin beneath the Neogene Pannonian Basin: a geodynamic model: Tectonophysics, 226, p. 433-455.

Tari, G., Dövényi, P., Dunkl, I., Horváth, F., Lenkey, L., Stefanescu, M., Szafián, P., and Tóth, T., 1999, Lithospheric Structure of the Pannonian basin derived from seismic, gravity and geothermal data. – In: Durand, B. Jolivet, L., Horváth, F., Séranne, M. (eds): The Mediterranean Basins: Tertiary Extension within the Alpine Orogen: Geol. Soc. London, Spec. Publ., 156, p. 215-250.

von Eynatten, H., Pawlowsky-Glahn, V. and Egozcue, J. J., 2002, Understanding perturbation on the simplex: a simple method to better visualise and interpret compositional data in ternary diagrams. Mathematical Geology, 34, p. 246-258.

von Eynatten, H., Barceló-Vidal, C., and Pawlowsky-Glahn, V., 2003a, Composition and discrimination of sandstones: a statistical evaluation of different analytical methods: Journal of Sedimentary Research, 73, p. 47-57.

von Eynatten, H., Barceló-Vidal, C., and Pawlowsky-Glahn, V., 2003b, Modelling compositional change: the example of chemical weathering of granitoid rocks: Mathematical Geology, 35, p. 231-251.